

SHORT COMMUNICATION

Atypical E2Fs inhibit tumor angiogenesis

BGMW Weijts^{1,2,7}, B Westendorp^{1,7}, BT Hien¹, LM Martínez-López¹, M Zipp¹, I Thurlings¹, RE Thomas¹, S Schulte-Merker^{3,4}, WJ Bakker^{1,5} and A de Bruin^{1,6}

Atypical E2F transcription factors (E2F7 and E2F8) function as key regulators of cell cycle progression and their inactivation leads to spontaneous cancer formation in mice. However, the mechanism of the tumor suppressor functions of E2F7/8 remain obscure. In this study we discovered that atypical E2Fs control tumor angiogenesis, one of the hallmarks of cancer. We genetically inactivated atypical E2Fs in epithelial and mesenchymal neoplasm and analyzed blood vessel formation in three different animal models of cancer. Tumor formation was either induced by application of 7,12-Dimethylbenz(a)anthracene/12-O-Tetradecanoylphorbol-13-acetate or by Myc/Ras overexpression. To our surprise, atypical E2Fs suppressed tumor angiogenesis in all three cancer models, which is in a sharp contrast to previous findings showing that atypical E2Fs promote angiogenesis during fetal development in mice and zebrafish. Real-time imaging in zebrafish displayed that fluorescent-labeled blood vessels showed enhanced intratumoral branching in xenografted *E2f7/8*-deficient neoplasms compared with *E2f7/8*-proficient neoplasms. DLL4 expression, a key negative inhibitor of vascular branching, was decreased in *E2f7/8*-deficient neoplastic cells, indicating that E2F7/8 might inhibit intratumoral vessel branching via induction of DLL4.

Oncogene (2018) 37, 271–276; doi:10.1038/onc.2017.336; published online 18 September 2017

INTRODUCTION

During development, the formation of new blood vessels (vasculogenesis) and blood vessels derived thereof (angiogenesis) is a tightly regulated process, resulting in a quiescent stable vasculature composed of arterioles, venules and capillaries.¹ Angiogenesis can be transiently induced from this quiescent vasculature, for example, during wound healing.² During tumor development, however, angiogenesis is almost continuously turned on, enabling tumor progression.³ The unstable, leaky and highly unorganized tumor vasculature not only gains access to oxygen and nutrients, but also provides a way for cancer cells to disseminate to distal organs.^{2,3} In this light, angiogenic therapies that normalize tumor vasculature have been put forward, as they relieve tumor hypoxia and inhibit metastasis,^{4,5} and could also improve the efficacy of radiotherapy, chemotherapy and immunotherapy.⁵

The E2F family of transcription factors consists of eight genes, which encode proteins that are generally classified either as activator (E2F1–E2F3) or repressor (E2F4–8).^{6,7} E2F factors are key regulators of the cell cycle,^{6,7} and therefore suspected regulators of human cancer. E2F amplification, overexpression or deletion is observed in a wide array of human cancers,⁸ although the exact contribution of these events to cancer is largely unknown. Studies in mice however point to dual roles for E2Fs in tumor development, suggesting that the role of E2Fs in cancer may be cell type specific, and may depend on the oncogenic background.⁸

The atypical E2Fs, E2F7 and E2F8 (E2F7/8), are unique members of the E2F family of transcription factors as they contain two instead of one DNA binding domain, lack a Retinoblastoma and Dimerization Partner domain, and instead form hetero- or homodimers.^{6,9} Interestingly, although E2Fs are key regulators of the cell cycle, embryonically lethal *E2f7/8* double-knockout (DKO) mice do not display significant proliferative defects, but instead display vascular defects and widespread apoptosis, demonstrating critical functions for E2F7/8 beyond proliferation.⁹ Intriguingly, recent findings suggest a role for E2F7/8 in human cancer. For example, deregulation of *E2F7/8* is observed in various cancers.⁸ And although E2F7/8 are classified as transcriptional repressors, suggesting tumor suppressive functions, E2F8 was found to be overexpressed in human lung and hepatocellular carcinoma, and to promote tumor growth of human lung and liver cancer cells in xenograft studies.^{10,11} However, recent studies from our lab did reveal tumor suppressive roles for E2F7/8 in mouse models of liver and skin cancer. We demonstrated that conditional deletion of *E2f7/8* in hepatocytes resulted in spontaneous formation of hepatocellular carcinomas and loss of *E2f7/8* in keratinocytes accelerated carcinogen-induced squamous cell carcinoma formation.^{12,13} However, the biological mechanisms through which E2F7/8 control tumor development are largely unknown. As tumor angiogenesis represents one of the hallmarks of cancer and atypical E2Fs regulate developmental angiogenesis,^{9,14} here we investigated a potential role for E2F7/8 in tumor angiogenesis, utilizing mouse and zebrafish models of cancer. We discovered that cancer cell-specific loss of atypical E2Fs

¹Department of Pathobiology, Faculty of Veterinary Medicine, Utrecht University, Utrecht, The Netherlands; ²Department of Cellular and Molecular Medicine, University of California-San Diego, La Jolla, CA, USA; ³Hubrecht Institute, Royal Netherlands Academy of Arts and Sciences and University Medical Center Utrecht, Utrecht, The Netherlands; ⁴Institute for Cardiovascular Organogenesis and Regeneration, Cells-in-Motion Cluster of Excellence, University of Münster, Münster, Germany; ⁵Department of Dermatology, Academic Medical Center, University of Amsterdam, Amsterdam, The Netherlands and ⁶Department of Pediatrics, Division of Molecular Genetics, University Medical Center Groningen, University of Groningen, Groningen, The Netherlands. Correspondence: Dr WJ Bakker or Professor Dr A de Bruin, Laboratory of Experimental Dermatology, Academic Medical Center – UvA, Room L3-119, Meibergdreef 9, 1105 AZ Amsterdam, The Netherlands.

E-mail: w.j.bakker@amc.uva.nl or a.debruin@uu.nl

⁷These authors contributed equally to this work.

Received 30 January 2017; revised 11 July 2017; accepted 11 July 2017; published online 18 September 2017

enhances tumor angiogenesis and branching of tumor blood vessels.

RESULTS AND DISCUSSION

E2f7/8-deficient skin tumors display enhanced angiogenesis

Recently, we demonstrated that keratinocyte-specific deletion of *E2f7/8* enhances tumor growth and aggressiveness in a two-stage mouse skin carcinogenesis model.¹³ In this model, skin tumors were induced in wildtype (WT) and keratinocyte-specific *E2f7/8* DKO mice by painting the back skin with application of 7,12-Dimethylbenz(a)anthracene and 12-O-Tetradecanoylphorbol-13-acetate. To investigate if E2F7/8 regulate tumor angiogenesis in these skin tumors, we performed immunohistochemical staining for Factor VIII, an established marker for blood vessels, in control and keratinocyte-specific *E2f7/8* DKO papillomas. This analysis revealed enhanced tumor angiogenesis in *E2f7/8* DKO versus WT papillomas (Figures 1a and b). A similar trend was observed in squamous cell carcinomas (not shown). Because transcriptional control of *E2f1* is a key mechanism through which E2F7/8 regulate developmental processes, as shown for apoptosis⁹ and liver polyploidization,¹⁵ and because *E2f1* itself regulates tumor angiogenesis^{16–18} and its expression was increased in *E2f7/8* DKO papillomas (Figure 1c), we next explored if E2F7/8 regulate tumor vascularization in an E2F1-dependent manner. For this purpose tumor angiogenesis was examined in *E2f1/7/8* triple knockout (TKO) papillomas. Notably, Factor VIII staining of TKO papillomas revealed that additional deletion of *E2f1* did not significantly change the extent of tumor angiogenesis compared with DKO papillomas (Figures 1a and b). Therefore we conclude that E2F7/8 regulate angiogenesis during papilloma formation independent of E2F1, although it cannot be excluded that its loss is compensated for by other activator E2Fs.

Recently, we showed that E2F7/8, in cooperation with HIF1, control vascular development through direct transcriptional stimulation of *VEGFA*,¹⁴ and motor neuron development through direct transcriptional repression of *NRP1*.¹⁹ As *VEGFA* and *NRP1* both regulate embryonic and tumor angiogenesis,^{20,21} E2F7/8 may regulate tumor angiogenesis through transcriptional control of these genes. Therefore we explored if *Vegfa* and *Nrp1* mRNA levels were deregulated in the *E2f7/8* DKO papillomas. However, despite the fact that we could confirm the stimulatory role of E2F7/8 in *Vegfa* expression in two primary keratinocyte cell lines *in vitro* (Supplementary Figures S1a, b), *Vegfa* and *Nrp1* mRNA levels were not significantly changed in *E2f7/8* DKO papillomas (Figure 1c), while the E2F7/8 repressed target *E2f1*⁹ was significantly increased, confirming functional *E2f7/8* deletion (Figure 1c). These data therefore show that E2F7/8 inhibit papilloma vascularization, and likely do so independent of VEGFA and NRP1.

Loss of E2F7/8 in *Myc/Ras*-induced sarcomas promotes tumor angiogenesis

To determine whether E2F7/8 can regulate tumor angiogenesis in a different oncogenic setting, we transformed WT and *E2f7/8* DKO mouse embryonic fibroblasts (MEFs) with the *Myc* and *Ras* oncogenes, hereafter referred to as control MEFs and *E2f7/8* DKO MEFs, respectively (Supplementary Figure S2). MEFs were grafted subcutaneously into athymic nude mice (Figure 2a). Microscopic analysis showed that the morphology did not differ between control and *E2f7/8* DKO sarcomas (Figure 2b). To analyze the amount of angiogenesis within the grafts, we assessed the influx of endothelial cells (ECs) from the host into solid tumor mass. To this end, ECs were labeled with fluorescent Isolectin B4, an EC-specific marker, and were quantified by confocal microscopy. Similar to the skin cancer model, we found a marked increase in the number of ECs in *E2f7/8* DKO compared with

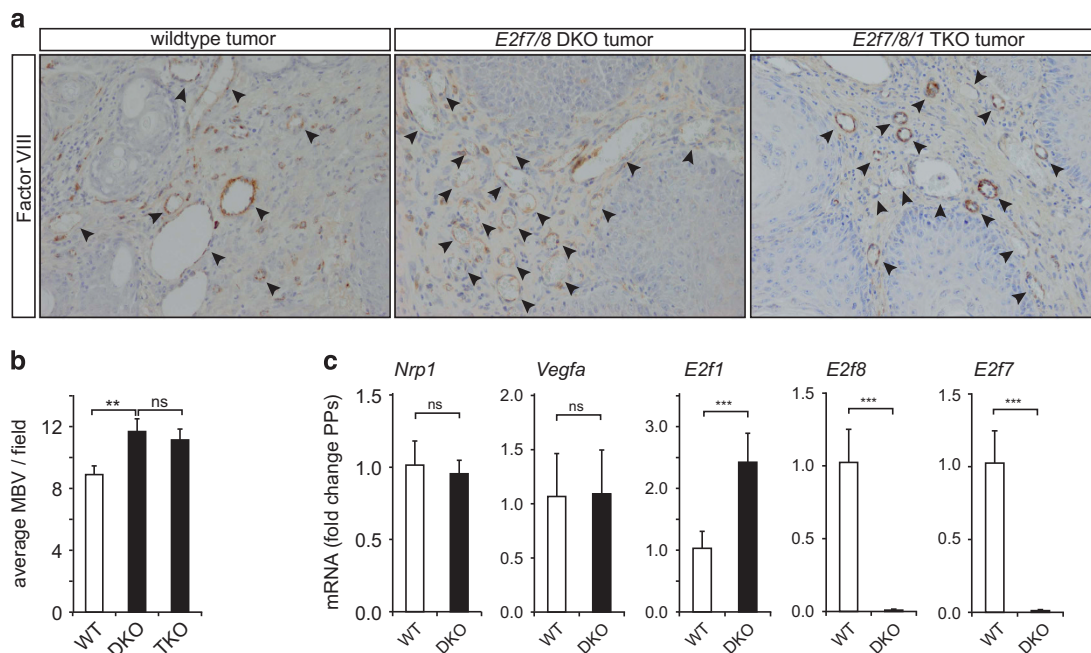


Figure 1. E2F7/8 repress tumor angiogenesis in a two-stage skin carcinogenesis model. **(a)** Immunohistochemical staining for Factor VIII in wildtype (WT), *E2f7/8* double knockout (DKO) or *E2f7/8/1* triple knockout (TKO) papillomas. Papillomas were obtained from a previously performed two-stage (application of 7,12-Dimethylbenz(a)anthracene/12-O-Tetradecanoylphorbol-13-acetate) skin carcinogenesis study.¹³ The brown staining shows factor VIII positive cells. Arrows indicate micro blood vessels (MBV) in each genetic group. **(b)** Quantification of MBV as depicted in **(a)**. MBV were counted in 25, 21 and 13 fields in wildtype, DKO and TKO papillomas, respectively. Wildtype and DKO papillomas were harvested from six mice, TKO from three mice. Quantified data present the average \pm s.e.m. **(c)** qPCR analysis of *Nrp1a*, *Vegfa*, *E2f1*, *E2f7* and *E2f8* mRNA levels analyzed in wildtype ($n = 6$) and DKO ($n = 9$) papillomas. Quantified data present the average \pm s.d. compared with the indicated controls. ** $P < 0.01$; *** $P < 0.001$; ns, not significant.

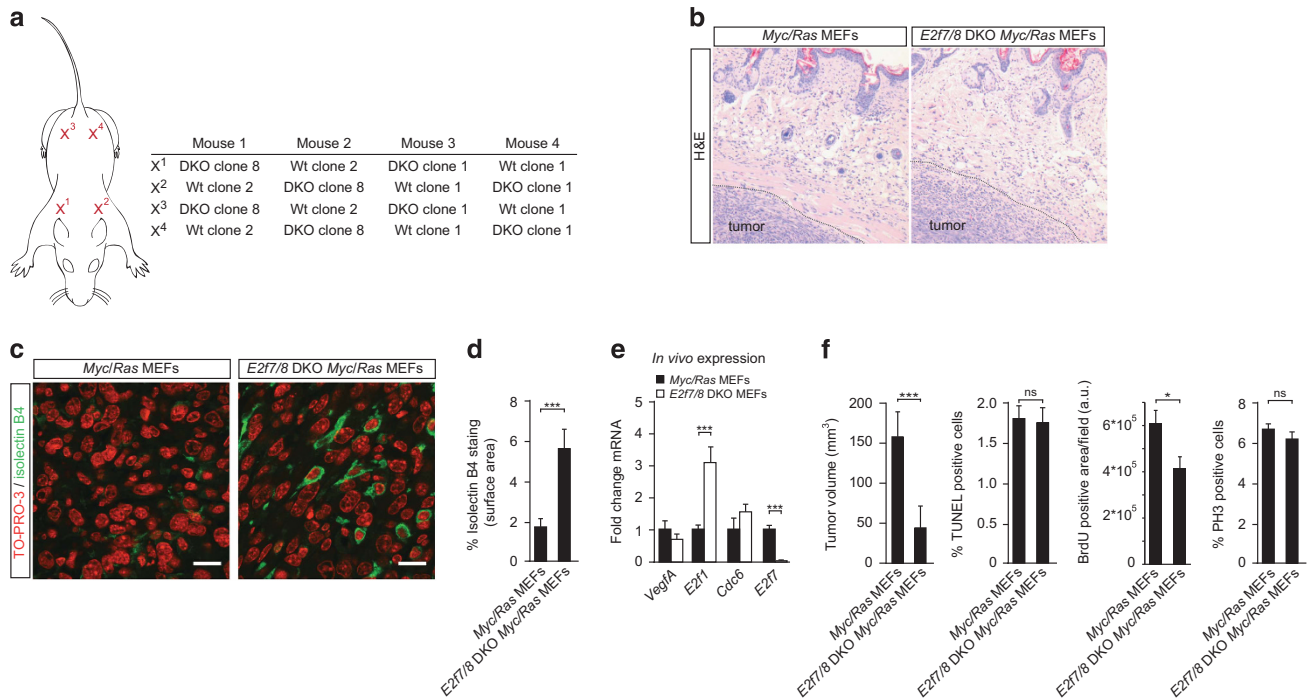


Figure 2. Absence of *E2f7/8* in mouse xenograft tumors leads to increased tumor vascularization. **(a)** Schematic representation of xenograft positions and experimental setup. MEFs were injected with a total of one million cells subcutaneously into athymic nude mice. The diameter of the tumors was monitored every 2 days. After 8 days, when the first tumors reached a diameter of 1 cm, all mice were euthanized and tumors harvested. **(b)** Hematoxylin and eosin (H&E) staining of control and *E2f7/8* DKO xenograft tumors. Dashed black line indicates tumor border. **(c)** Staining and quantification **(d)** of intratumoral endothelial cell (Isolectin B4) and nuclei (TO-PRO-3) of control and *E2f7/8* DKO xenograft tumors ($n = 8$ tumors per genotype). For each tumor, five fields ($\times 400$ magnification) were quantified. White scale bars in **(c)** indicate 10 μm . **(e)** Messenger RNA expression of *Vegfa*, *E2f1*, *Cdc6* and *E2f7* in harvested *E2f7/8* DKO and control xenografted MEF tumors ($n = 8$ tumors per genotype). Quantitative PCR analysis was used to analyze mRNA levels. Messenger RNA levels in *E2f7/8* DKO tumors are depicted compared with control tumors. **(f)** Quantification (similar as in **(d)**) of tumor volume, *in vivo* BrdU incorporation, and phospho-histone 3 (PH3)-positive and TUNEL-positive cells as determined in the outer border zone of control and *E2f7/8* DKO xenograft tumors. All quantified data present the average \pm s.e.m. compared with the indicated controls. * $P < 0,05$; *** $P < 0,005$; ns, not significant; a.u., arbitrary units.

control tumors (Figures 2c and d). We also found reduced *Vegfa* mRNA levels (and increased *E2f1* mRNA levels) in *E2f7/8* DKO tumors (Figure 2e). From these data we conclude that *E2f7/8* also inhibit tumor angiogenesis in a xenograft model for sarcomas driven by *Myc* and *Ras* oncogenes, and again likely do so independent of *Vegfa* which levels are reduced. To test if the enhanced tumor angiogenesis in *E2f7/8* DKO tumors could result from enhanced EC migration (influx), an *in vitro* scratch assay was performed.²² In this experiment we assessed the potential of either *E2f7/8* DKO and control MEFs-conditioned medium to close a scratch made in a confluent layer of human umbilical cord vein endothelial cells (HUVECs). HUVECs cultured in *E2f7/8* DKO-conditioned medium showed a decreased closure of the scratch compared with controls (supplementary Fig. S3a, b). Similar results were obtained when HUVECs were replaced with WT MEFs or mouse embryonic ECs (not shown). These data suggest that loss of *E2F7/8* does not stimulate tumor angiogenesis by enhanced secretion of a factor that stimulates endothelial migration.

Although we previously demonstrated that genetic ablation of *E2f7/8* enhances tumor growth in a carcinogen-induced skin cancer model,¹³ in this study *E2f7/8* DKO MEF tumors were instead significantly smaller compared with controls (Figure 2f). And although *E2F7/8* are critical regulators in preventing apoptosis *in vivo*,⁹ which could explain the reduced tumor size, quantification of terminal deoxynucleotidyl transferase dUTP nick end labeling-positive cells revealed a comparable incidence of apoptosis between control and *E2f7/8* DKO grafts (Figure 2f). Therefore we next tested if tumor proliferation was affected.

Strikingly, *in vivo* BrdU incorporation studies demonstrated a significant reduction in DNA replication in *E2f7/8* DKO tumors, while staining of tumor sections with the mitosis marker phospho-histone 3 did not show differences between control and *E2f7/8* DKO tumors (Figure 2f). This indicates that *E2f7/8* DKO tumors proliferate slower, which likely contributes to their reduced size. Notably, mice deficient for activator E2Fs also have a delayed cell cycle progression.²³ Importantly, although the growth rate of *E2f7/8* DKO tumors was delayed (Figure 2f), the growth of *E2f7/8* DKO MEFs *in vitro* was not delayed (Supplementary Figure S2a-b), arguing for a role of the tumor microenvironment. In this regard it is interesting to mention that the subcutaneous space, in which the MEFs are engrafted, is relatively poorly vascularized, and that transplanted tumors depend on HIF1 for their growth in this relatively hypoxic environment.²⁴ And because *E2F7/8* are critical mediators of HIF functions *in vivo*,^{14,19} *E2F7/8* may be required to support the growth of subcutaneously engrafted, hypoxic tumors. In response to genotoxic stress, however, *E2F7/8* may limit the growth of tumors as we observed that *E2f7/8* DKO skin tumors are larger in carcinogen-induced skin cancer.¹³ However, future experiments are required to address if *E2F7/8* indeed differentially affect cellular proliferation in response to hypoxic or genotoxic stress, and whether this occurs in a HIF1-dependent manner. Another factor that could explain why *E2f7/8* DKO papillomas are larger,¹³ and transplanted *E2f7/8* DKO MEFs tumors smaller than their controls, may be the fact that *E2f7/8* DKO papillomas benefit for 3 months from the increased tumor vascularization, whereas this is only eight days in the *E2f7/8* DKO MEF tumors (Figure 2).

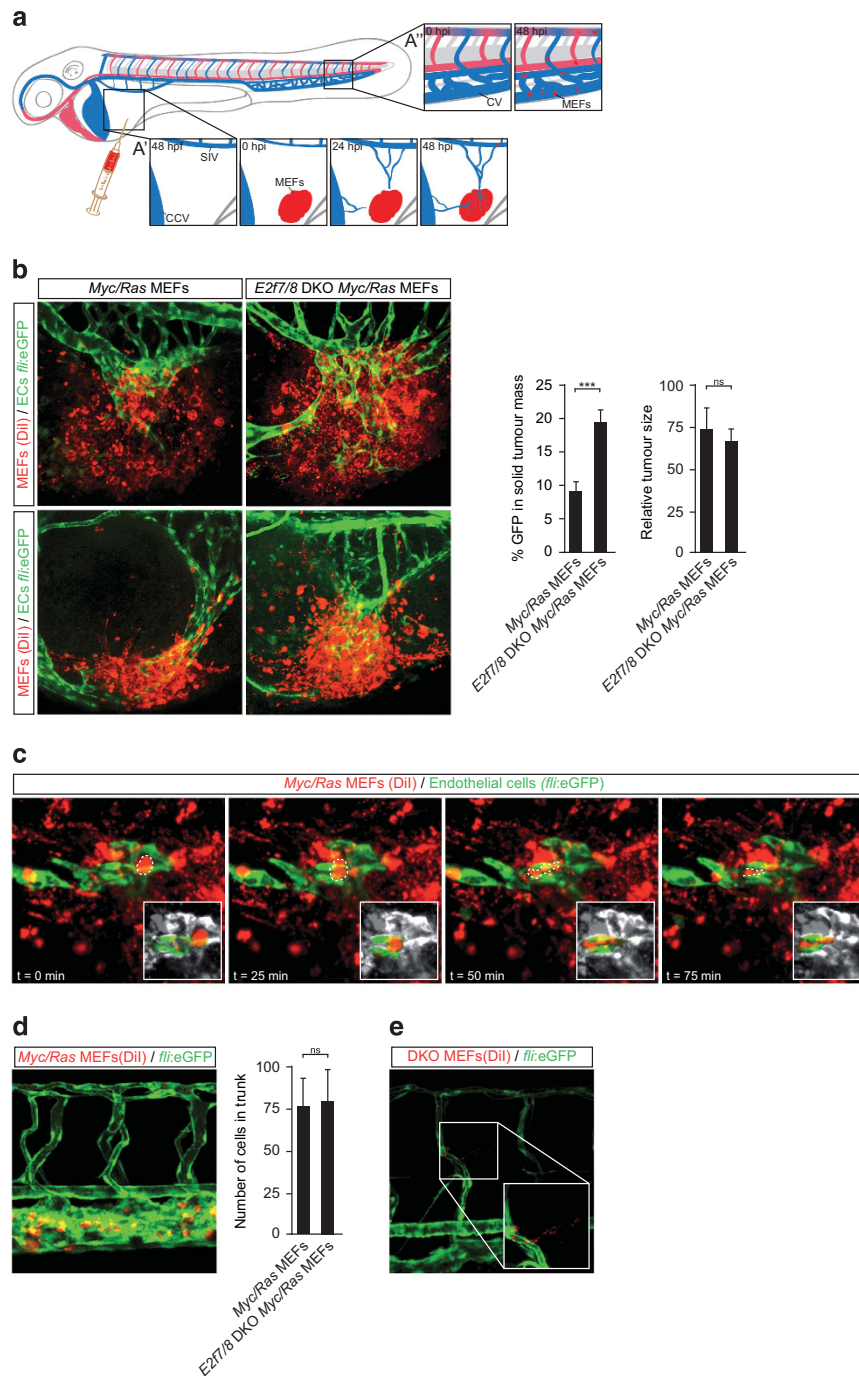


Figure 3. Absence of *E2f7/8* in zebrafish xenograft tumors leads to increased tumor vascularization. **(a)** Schematic representation of xenograft positions and experimental setup. Labeled MEFs were injected 48 h post fertilization (hpf) in the perivitelline space on the yolk sac, ventrally of the sub intestinal vein (SIV) and posteriorly of the common cardinal vein (CCV or duct of Cuvier). Grafts tend to evoke an angiogenic response from the SIV, but frequently also from the CCV (3a'). In addition, neoplastic cells from the injection site are able to enter the circulation via the vessels formed by tumor angiogenesis and often attach or simply get stuck in the caudal vein (CV) region (3a''). Reprinted with permission from Magliozzi, R. *et al.*³¹ **(b)** Representative images and quantification of tumor angiogenesis and size of control (Red; Dil; $n = 10$) and *E2f7/8* DKO tumors (Red; Dil; $n = 10$) injected in *Tg(fli1a:gfp)* zebrafish. **(c)** Time-lapse series that shows metastasizing cell (dashed line) from the tumor into the vasculature. Insets display metastasizing cell only. **(d)** Representative image and quantification of MEFs metastasis in the trunk region. **(e)** Example of extravasation of (*E2f7/8* DKO) MEFs into the surrounding tissue. Abbreviations: CV, caudal vein; CCV, common cardinal vein; hpi, hours post injection. All quantified data present the average \pm s.d. compared with the indicated controls in at least three independent experiments. $***P < 0.05$; ns, not significant.

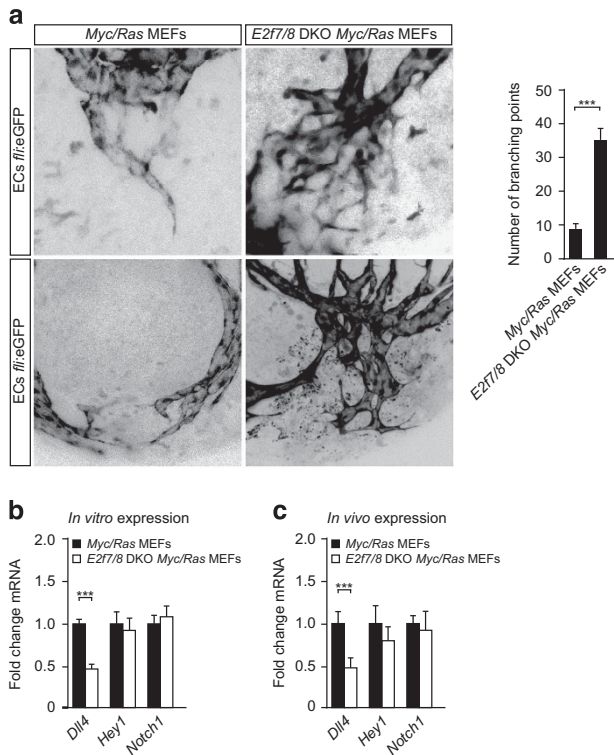


Figure 4. Loss *E2f7/8* in xenografted MEF tumors in zebrafish leads to increased intratumoral blood vessel branching. Experimental setup similar as described in Figure 3a. (a) Representative image and quantification ($n = 10$) of hyperbranching in control and *E2f7/8* DKO tumors injected in *Tg(fli1a:gfp)* (black color; endothelial cells). (b) Indicated mRNA levels measured in control or *E2f7/8* DKO MEFs cultured under standard conditions using qPCR. (c) Indicated mRNA levels measured in zebrafish xenografts of control (eight tumors) or *E2f7/8* DKO MEFs (five tumors). All quantified data present the average \pm s.d. compared with the indicated controls. *** $P < 0.05$; ns, not significant.

Inactivation of *E2F7/8* stimulates hyperbranching of intratumoral blood vessels and decreases *DLL4* expression

To investigate the tumor angiogenesis phenotype of *E2f7/8*-deficient tumors in more detail, we grafted Ras/Myc transformed control and *E2f7/8* DKO MEFs into *Tg(fli1:eGFP)* zebrafish, in which endothelial cells (ECs) are labeled green. We used this xenograft zebrafish model to monitor in real-time tumor angiogenesis, and the dissemination and metastasis of neoplastic cells (Figure 3a).²⁵ In line with the skin cancer and mouse xenograft tumor models, *E2f7/8* DKO MEFs grafts triggered an increased influx of ECs, quantified as the amount of GFP signal within the boundaries of the tumor 48 h post injection (hpi) (Figure 3b). Tumor size measurements revealed that *E2f7/8* DKO MEFs grafts were comparable to controls (Figure 3b). This is consistent with the absence of either genotoxic and hypoxic stress in this model. Furthermore, time-lapse imaging showed a continuous movement of tumor cells within the graft and, in addition, cells entering EC (GFP-positive) tube-like structures (Figure 3c, and supplementary movie). Metastatic cells were detected throughout the fish 48 hpi, but within the existing circulatory system and with increased density in the caudal vein (CV, Figure 3d). However, quantification of the number of cells present in the CV 48 hpi showed no difference in metastatic rate between *E2f7/8* DKO compared with control MEFs (Figure 3d). Of note, we sporadically detected cells outside the vasculature (Figure 3e). These cells could give rise to metastases, although we cannot exclude the possibility that these Dil- or DiD-positive cells are macrophages that have scavenged

fluorescent cell debris or phagocytized MEFs. Therefore we conclude that the absence of *E2F7/8* in this xenograft zebrafish model does not impact the dissemination of neoplastic cells, but does enhance tumor angiogenesis, consistent with the findings from the mouse tumor studies (Figures 1 and 2).

Enhanced tumor angiogenesis can result not only from advanced capillary sprouting, but also from excessive vessel branching.³ For this reason we quantified the number of intratumoral blood vessel branching points in the zebrafish xenograft model. Notably, blood vessels in *E2f7/8* DKO tumors show an almost four times higher number of branching points compared with control tumors (Figure 4a). As the Delta-like 4 (*DLL4*)-Notch pathway is a key regulator of blood vessel branching during developmental and tumor angiogenesis,^{26,27} we tested whether components of this pathway were deregulated. We found that deletion of *E2f7/8* both *in vitro* and in engrafted tumors, resulted in decreased expression of the Notch ligand *Dll4*, and of the *Dll4*/Notch1 target *Hey1*, however the latter did not reach statistical significance (Figures 4b and c). The observed increase in tumor angiogenesis upon *E2f7/8* deletion is in line with the decreased expression of *Dll4*, as *Dll4* is known to have a repressive function in blood vessel branching.¹ Similar to the mouse tumor xenografts, *Vegfa* mRNA levels in the grafts were reduced (data not shown).

These data suggest that *E2F7/8* regulate vessel branching through direct or indirect control of *DLL4* expression. This hypothesis is supported by the observed decrease in *Dll4* mRNA levels in cultured *E2f7/8* DKO MEFs before grafting into animals (Figure 4b), and by the observation that multiple E2Fs (*E2F1/4/6*) bind the *DLL4* promoter in various cell types (Supplementary Figure S4). Direct transcriptional control of the *DLL4* locus by *E2F7/8* seems unlikely as *DLL4* was not identified in two recent chromatin immunoprecipitation-seq analysis for *E2F7* (supplementary Fig. S4).^{19,28} Although we recently identified *E2F6* as a potential *E2F7/8* target,^{19,28} *E2F6* mRNA and protein levels were not deregulated in *E2f7/8* DKO MEFs (not shown). Therefore it is unlikely that *E2F7/8* control *DLL4* expression indirectly through *E2F6*.

Alternatively, the induction of *E2F1* upon loss of *E2F7/8* may reduce *DLL4* expression through inhibition of HIF1. Namely, HIF1 has been reported to stimulate *DLL4* expression,²⁹ and to bind the *DLL4* promoter (Supplementary Figure S4), whereas our previous data suggests competitive promoter binding between *E2F1* and HIF1 α ,¹⁹ and reduced HIF1 α protein levels upon overexpression of *E2F1* (data not shown).

In conclusion, using three different tumor models, we have identified *E2F7/8* as inhibitors of tumor angiogenesis (Figures 1b, 2d, 3b). And although we recently reported that *E2F7/8* regulate developmental angiogenesis through transcriptional stimulation of *VEGFA* in cooperation with HIF1,¹⁴ this study strongly suggests that *E2F7/8* regulate tumor angiogenesis independent of *VEGFA*, as we observed reduced *Vegfa* mRNA levels in *E2f7/8* DKO MEFs (Supplementary Figure S2c), keratinocytes (Supplementary Figure S1b), and in engrafted tumors (Figure 2e), whereas tumor angiogenesis was enhanced in all three tumor models. Instead we found that *E2F7/8* affect tumor angiogenesis at least in part through control of vessel branching, possibly through indirect control of *DLL4* expression. However, we expect that this does not present a general mechanism of how *E2F7/8* mediate tumor angiogenesis, as *Dll4* expression was not deregulated in *E2f7/8*-deficient mouse papillomas (Supplementary Figure S1c). *E2F7/8* may therefore mediate tumor angiogenesis through multiple mechanisms. Consistent with this notion is our previous observation that a variety of angiogenic factors are deregulated in *E2f7/8*-deficient mouse embryos and placentas.³⁰ In line with the increasing understanding of E2Fs as genetic and cellular context-dependent factors, *E2F7/8* may thus affect tumor angiogenesis in a context-dependent manner, as previously

suggested for other players of the E2F pathway.³⁰ Therefore it will be valuable to decipher these context-dependent mechanisms via which E2F7/8 mediate tumor angiogenesis and development, in order to fully understand the versatile role of E2F7/8 in cancer.

CONFLICT OF INTEREST

The authors declare no conflict of interest.

ACKNOWLEDGEMENTS

This study was financially supported by grants from the Dutch Cancer Society (UU2009–4353) to WJB, and (UU2013–5777) to BW and AdB. From the Association of International Cancer Research (09–0718) to WJB, and from the Netherlands Organization for Scientific Research (NWO-ALW 11-28) to AdB.

REFERENCES

- Adams RH, Alitalo K. Molecular regulation of angiogenesis and lymphangiogenesis. *Nat Rev Mol Cell Biol* 2007; **8**: 464–478.
- Chung AS, Lee J, Ferrara N. Targeting the tumour vasculature: insights from physiological angiogenesis. *Nat Rev Cancer* 2010; **10**: 505–514.
- Hanahan D, Weinberg RA. Hallmarks of cancer: the next generation. *Cell* 2011; **144**: 646–674.
- Goel S, Duda DG, Xu L, Munn LL, Boucher Y, Fukumura D *et al*. Normalization of the vasculature for treatment of cancer and other diseases. *Physiol Rev* 2011; **91**: 1071–1121.
- Jain RK. Antiangiogenesis strategies revisited: from starving tumors to alleviating hypoxia. *Cancer Cell* 2014; **26**: 605–622.
- DeGregori J, Johnson DG. Distinct and overlapping roles for E2F family members in transcription, proliferation and apoptosis. *Curr Mol Med* 2006; **6**: 739–748.
- Dimova DK, Dyson NJ. The E2F transcriptional network: old acquaintances with new faces. *Oncogene* 2005; **24**: 2810–2826.
- Chen HZ, Tsai SY, Leone G. Emerging roles of E2Fs in cancer: an exit from cell cycle control. *Nat Rev Cancer* 2009; **9**: 785–797.
- Li J, Ran C, Li E, Gordon F, Comstock G, Siddiqui H *et al*. Synergistic function of E2F7 and E2F8 is essential for cell survival and embryonic development. *Dev Cell* 2008; **14**: 62–75.
- Deng Q, Wang Q, Zong WY, Zheng DL, Wen YX, Wang KS *et al*. E2F8 contributes to human hepatocellular carcinoma via regulating cell proliferation. *Cancer Res* 2010; **70**: 782–791.
- Park SA, Platt J, Lee JW, Lopez-Giraldez F, Herbst RS, Koo JS. E2F8 as a novel therapeutic target for lung cancer. *J Natl Cancer Inst* 2015; **107**: 10.1093/jnci/djv151. Print 2015 Sep.
- Kent LN, Rakijas JB, Pandit SK, Westendorp B, Chen HZ, Huntington JT *et al*. E2f8 mediates tumor suppression in postnatal liver development. *J Clin Invest* 2016; **126**: 2955–2969.
- Thurlings I, Martinez-Lopez LM, Westendorp B, Zijp M, Kuiper R, Tooten P *et al*. Synergistic functions of E2F7 and E2F8 are critical to suppress stress-induced skin cancer. *Oncogene* 2017; 829–839.
- Weijts BG, Bakker WJ, Cornelissen PW, Liang KH, Schaftenaar FH, Westendorp B *et al*. E2F7 and E2F8 promote angiogenesis through transcriptional activation of VEGFA in cooperation with HIF1. *EMBO J* 2012; **31**: 3871–3884.
- Pandit SK, Westendorp B, Nantasanti S, van Liere E, Tooten PC, Cornelissen PW *et al*. E2F8 is essential for polyploidization in mammalian cells. *Nat Cell Biol* 2012; **14**: 1181–1191.

- Merdzhanova G, Gout S, Keramidas M, Edmond V, Coll JL, Brambilla C *et al*. The transcription factor E2F1 and the SR protein SC35 control the ratio of pro-angiogenic versus antiangiogenic isoforms of vascular endothelial growth factor-A to inhibit neovascularization in vivo. *Oncogene* 2010; **29**: 5392–5403.
- Qin G, Kishore R, Dolan CM, Silver M, Wecker A, Luedemann CN *et al*. Cell cycle regulator E2F1 modulates angiogenesis via p53-dependent transcriptional control of VEGF. *Proc Natl Acad Sci USA* 2006; **103**: 11015–11020.
- Fontemaggi G, Dell'Orso S, Trisciuglio D, Shay T, Melucci E, Fazi F *et al*. The execution of the transcriptional axis mutant p53, E2F1 and ID4 promotes tumor neo-angiogenesis. *Nat Struct Mol Biol* 2009; **16**: 1086–1093.
- de Bruin A, A Cornelissen PW, Kirchmaier BC, Mokry M, Ilich E, Nirmala E *et al*. Genome-wide analysis reveals NRP1 as a direct HIF1alpha-E2F7 target in the regulation of motoneuron guidance in vivo. *Nucleic Acids Res* 2016; **44**: 3549–3566.
- Raimondi C, Ruhrberg C. Neuropilin signalling in vessels, neurons and tumours. *Semin Cell Dev Biol* 2013; **24**: 172–178.
- Djordjevic S, Driscoll PC. Targeting VEGF signalling via the neuropilin co-receptor. *Drug Discov Today* 2013; **18**: 447–455.
- Liang CC, Park AY, Guan JL. In vitro scratch assay: a convenient and inexpensive method for analysis of cell migration in vitro. *Nat Protoc* 2007; **2**: 329–333.
- Chen D, Pacal M, Wenzel P, Knoepfler PS, Leone G, Bremner R. Division and apoptosis of E2f-deficient retinal progenitors. *Nature* 2009; **462**: 925–929.
- Blouw B, Song H, Tihan T, Bosze J, Ferrara N, Gerber HP *et al*. The hypoxic response of tumors is dependent on their microenvironment. *Cancer Cell* 2003; **4**: 133–146.
- He S, Lamers GE, Beenakker JW, Cui C, Ghotra VP, Danen EH *et al*. Neutrophil-mediated experimental metastasis is enhanced by VEGFR inhibition in a zebrafish xenograft model. *J Pathol* 2012; **227**: 431–445.
- Noguera-Troise I, Daly C, Papadopoulos NJ, Coetzee S, Boland P, Gale NW *et al*. Blockade of Dll4 inhibits tumour growth by promoting non-productive angiogenesis. *Nature* 2006; **444**: 1032–1037.
- Hogan BM, Herpers R, Witte M, Helotera H, Alitalo K, Duckers HJ *et al*. Vegfc/Flt4 signalling is suppressed by Dll4 in developing zebrafish intersegmental arteries. *Development* 2009; **136**: 4001–4009.
- Westendorp B, Mokry M, Groot Koerkamp MJ, Holstege FC, Cuppen E, de Bruin A. E2F7 represses a network of oscillating cell cycle genes to control S-phase progression. *Nucleic Acids Res* 2012; **40**: 3511–3523.
- Diez H, Fischer A, Winkler A, Hu CJ, Hatzopoulos AK, Breier G *et al*. Hypoxia-mediated activation of Dll4-Notch-Hey2 signaling in endothelial progenitor cells and adoption of arterial cell fate. *Exp Cell Res* 2007; **313**: 1–9.
- Bakker WJ, Weijts BG, Westendorp B, de Bruin A. HIF proteins connect the RB-E2F factors to angiogenesis. *Transcription* 2013; **4**: 62–66.
- Magliozzi R, Low TY, Weijts BG, Cheng T, Spanjaard E, Mohammed S *et al*. Control of epithelial cell migration and invasion by the IKKbeta- and CK1alpha-mediated degradation of RAPGEF2. *Dev Cell* 2013; **27**: 574–585.



This work is licensed under a Creative Commons Attribution-NonCommercial-NoDerivs 4.0 International License. The images or other third party material in this article are included in the article's Creative Commons license, unless indicated otherwise in the credit line; if the material is not included under the Creative Commons license, users will need to obtain permission from the license holder to reproduce the material. To view a copy of this license, visit <http://creativecommons.org/licenses/by-nc-nd/4.0/>

© The Author(s) 2018

Supplementary Information accompanies this paper on the Oncogene website (<http://www.nature.com/onc>)